DOI: 10.1002/chem.200902531

Synthesis of Superacid-Functionalized Mesoporous Nanocages with Tunable Pore Diameters and Their Application in the Synthesis of Coumarins

Pranjal Kalita,[a] B. Sathyaseelan,[a] Ajayan Mano,[a] S. M. Javaid Zaidi,[b] Murugulla A. Chari,[a] and Ajayan Vinu*[a]

Abstract: Here we demonstrate for the first time the preparation of a triflic acid (TFA)-functionalized mesoporous nanocage with tunable pore diameters by the wet impregnation method. The obtained materials have been unambiguously characterized by XRD, N_2 adsorption, FTIR spectroscopy, and NH_3 temperature-programmed desorption (TPD). From the characterization results, it has been found that the TFA molecules are firmly anchored on the surface of the mesoporous supports without affecting their acidity. We also demonstrate the effect of the pore and cage diameter of the KIT-5 supports on the loading of TFA molecules inside the pore channels. It has been found that the total acidity of the materials increases with an increase in the TFA loading on the support, whereas the acidity of the materials decreases with an increase in the pore diameter of the support. The acidity of the TFA-functionalized mesoporous nanocages is much higher than that of the zeolites and metal-substituted mesoporous acidic catalysts. The TFA-functionalized materials have also been employed as the catalysts for the synthesis of 7-hydroxy-4-methylcoumarin by means of the Pechmann reaction under solvent-free conditions. It has been found that the catalytic activity of the TFA-functionalized KIT-5 is much higher than that of zeolites and metal-substituted mesoporous catalytic materials in the synthesis of coumarin derivatives. The stability of the catalyst is extremely good and can be reused several times without much loss of activity in the above reaction.

Keywords: heterogeneous catalysis · mesoporous materials · nanostructures · Pechmann reaction · resorcinol

Introduction

Mesoporous silica materials have recently been studied extensively due to their unique structures with organized porosity, high specific surface area, and specific pore volume, which make them available to a wide range of applications in the areas of adsorption, separation, sensing, and fuel cells.[1–18] Among the mesoporous materials, materials that consist of interconnected large-pore cage-type mesoporous systems with three-dimensional (3D) porous networks are highly interesting and promising supports for heterogeneous catalysis. In addition, they are considered to be more advantageous than porous materials that have a hexagonal pore structure with a unidimensional array of pores because they allow for a faster diffusion of reactants, avoid pore blockage, provide more adsorption sites, and can be used for processing large-sized molecules. SBA-16, SBA-1, and KIT-5 are a few examples of porous materials that possess a 3D cage-type porous structure.[9,11,12] Among them, KIT-5, discovered by Kleitz et al., is very interesting as it possesses a highly ordered cage-type mesoporous structure with a cubic *Fm*3*m* closely packed symmetry, a high surface area, a large cage-type tunable pore, and a high specific pore volume.[19] These exciting properties made it an excellent adsorbent for capturing large biomolecules as well as an ideal replica for the fabrication of cage-type carbon material.[20,21] However, KIT-5 materials possess low acidity and ion-exchange capability, which limit their application in catalysis.

To generate the acid functionality in the material, the pore or wall structure of the materials must be modified

[a] Dr. P. Kalita, B. Sathyaseelan, A. Mano, Dr. M. A. Chari, Dr. A. Vinu
International Center for Materials Nanoarchitectonics
World Premier International (WPI) Research Initiative
National Institute for Materials Science
Tsukuba, Ibaraki 305-0044 (Japan)
Fax: (81) 29 860 470 6
E-mail: vinu.ajayan@nims.go.jp

[b] Dr. S. M. J. Zaidi
Department of Chemical Engineering
King Fahd University of Petroleum and Minerals
Dhahran 31261 (Saudi Arabia)

either with trivalent metal ions by the direct synthesis method or by grafting the highly acidic homogenous catalyst or metal ions onto the surface of the pore walls by the post-synthetic method. Very recently, Vinu et al. reported the preparation of aluminum-supported mesoporous KIT-5 material (AlKIT-5), which possesses a 3D mesostructure with *Fm3m* symmetry and excellent textural characteristics.[17] Although the material showed excellent performance in the acid-catalyzed reactions, the acidity of the material is much lower than zeolites and zeotype materials. By increasing the acidity of the KIT-5 materials, the possibility of using the material as a catalyst for various acid-catalyzed organic transformations could be extended. To increase the acidity of the materials, which is critical for obtaining excellent performance in the various acid-catalyzed transformations, here we propose to modify the surface of the KIT-5 silica materials with one of the superacids, namely, trifluoromethanesulfonic acid (CF_3SO_3H), which is also called triflic acid (TFA). TFA is considered to be a strong Brønsted acid catalyst and its acid strength is much higher than that of the pure sulfuric acid due to the presence of the electron-withdrawing fluorine atoms attached to the sulfonic acid groups. As TFA possesses excellent acidic characteristics, it has been widely used in many acid-catalyzed transformations such as Friedel–Crafts reactions, polymerization, and Koch carbonylation. However, TFA is highly toxic, environmentally hazardous, and cannot be easily recovered from the product mixture. These problems can be overcome by the immobilization of the TFA on the solid supports.

Recently, Singh and co-workers reported the catalytic activity of TFA functionalized on mesoporous Zr-TMS material for versatile organic transformation reactions such as the acetalization of ethyl acetoacetate and the benzoylation of biphenyl.[22] Bennardi et al. reported the preparation of TFA-immobilized mesoporous titania and their application in the synthesis of flavones and chromones derivatives.[23] Unfortunately, the mesoporous support materials used in the above processes have poor textural parameters that limit the efficiency of the materials in the acid-catalyzed transformations. Although there are a few more reports available on the functionalization of TFA over mesoporous supports, most of them pertain to only 1D mesoporous supports.[24–26] To the best of our knowledge, there has been no report yet on the functionalization of TFA over 3D cage-type mesoporous support materials such as KIT-5. It should also be mentioned that the role of the pore diameter of the support materials on the functionalization of TFA molecules inside the porous channels of the cage-type materials has not been demonstrated in the open literature so far.

Coumarin and its derivatives occur widely in nature and most of them show biological activities such as anticoagulants, insecticides, cosmetics, optical brighteners, and dispersed fluorescent and laser dyes.[27–30] Coumarin can be synthesized by various "name reactions" using acidic as well as basic catalysts.[31–44] For example, 4-methyl-7-hydroxycoumarin has been prepared by the Pechmann reaction of a mixture of resorcinol (1,3-dihydroxybenzene) and ethyl acetoacetate (β-ketoester) and the use of various acidic catalysts such as sulfuric acid, zeolites, Nafion-H, and clays. Unfortunately, these catalysts suffer from one or more serious drawbacks such as poor textural characteristics, long reaction times, a stoichiometric amount of catalyst, and difficulties in catalyst recovery, drastic reaction conditions, low yields, and tedious workup procedures.

Here we report for the first time on the preparation and characterization of 3D mesoporous TFA-functionalized KIT-5 with different pore diameters and their application in the synthesis of coumarin by means of the Pechmann reaction of resorcinol (1,3-dihydroxybenzene) and ethyl acetoacetate (β-ketoester) (Scheme 1). We also demonstrate that

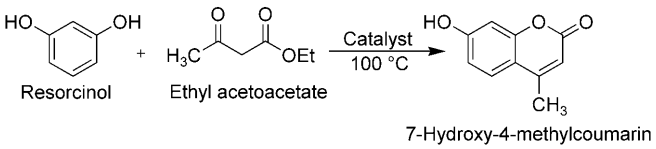

Scheme 1. Pechmann reaction between resorcinol and ethyl acetoacetate.

the amount of TFA on the surface of the KIT-5 can be controlled by the simple adjustment of the amount of TFA in the synthesis mixture. In addition, the effect of pore diameter of the KIT-5 support on the functionalization of TFA has also been demonstrated. All the catalytic materials have been characterized by nitrogen adsorption, XRD, FTIR spectroscopy, and ammonia temperature-programmed desorption (TPD). Moreover, the role of the amount of TFA and the pore diameter of the support, and the catalyst amount affecting the catalytic activity in the synthesis of 7-hydroxy-4-methylcoumarin has been demonstrated.

Results and Discussion

Initially, KIT-5 with different pore diameters was functionalized with different amounts of TFA by a postsynthetic wet impregnation method. The amount of TFA functionalization on the pore channels of the KIT-5 support was confirmed by scanning electron microscopy (SEM) energy-dispersive X-ray spectroscopy (EDX) analysis (not shown). EDX patterns of the all samples exhibit the peaks for C, O, F, Si, and S. The presence of the C, O, F, and S peaks, which originally come from the TFA molecules, indicates that the TFA molecules are indeed present inside the mesochannels of the KIT-5 support and bond with the surface silanol groups. EDX results also revealed that both the F and the S contents increase with an increase in the loading of TFA on the pore channels of the KIT-5(100), thus indicating that the TFA was successfully incorporated with the surface silanol groups on the pore channels of KIT-5(100).

The structure of the KIT-5 support after the TFA modification was confirmed by powder XRD measurements. Figure 1 shows the powder XRD patterns of the KIT-5(100) functionalized with different amounts of TFA. Purely sili-

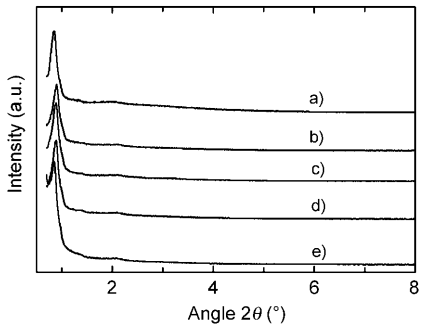

Figure 1. Powder XRD patterns of a) KIT-5(100), b) KIT-5(100)-5TA, c) KIT-5(100)-10TA, d) KIT-5(100)-15TA, and e) KIT-5(100)-20TA catalysts.

ceous KIT-5 exhibits three reflections in the region $2\theta = 0.7$ to 3°, which can be indexed to the (111), (200), and (220) reflections of the cubic space group *Fm*3*m*. The length of the cubic cell a_0 is calculated by using the formula $a_0 = d_{111}\sqrt{3}$ (Table 1). Interestingly, the structure of the KIT-5 was completely retained even after the modification of the pore surface of the KIT-5(100) with more than 20 wt% of TFA. However, the intensity of the (200) reflection in the XRD pattern of the KIT-5(100) sample decreases with an increase in the loading of TFA. This is mainly attributed to the occupation of the TFA molecules on the pore channels of the TFA. It should also be mentioned that the peaks are shifted towards the higher angle upon the functionalization of TFA molecules, thereby indicating the decrease in the *d* spacing and the unit-cell constant, as shown in Table 1. However, when the unit-cell parameters of the TFA-functionalized materials are compared, surprising results are found. The *d* spacing of the material increases with an increase in the loading of the TFA molecules over KIT-5(100) (Table 1) but is lower than the pristine KIT-5 support. We surmise that this could be due to the presence of the TFA molecules, which may change the diffraction of the X-rays. However, the exact reason for the huge reduction of the unit-cell constant of the KIT-5(100) functionalized with a lower amount of TFA is currently not known.

Table 1. Physicochemical characterization of KIT-5 samples.[a]

Catalysts	SA [$m^2 g^{-1}$]	a_o [nm]	PV [$cc g^{-1}$]	PD [nm]	CD [nm]
KIT-5(100)	700	18.1	0.44	5.8	10.80
KIT-5(130)	675	19.0	0.69	6.3	12.30
KIT-5(150)	470	20.67	0.75	7.4	13.50
KIT-5(100)-5TA	405	16.98	0.31	5.7	9.49
KIT-5(100)-10TA	390	17.14	0.30	5.7	9.50
KIT-5(100)-15TA	285	17.23	0.23	5.7	8.93
KIT-5(100)-20TA	240	17.92	0.22	5.7	9.17
KIT-5(130)-20TA	440	18.38	0.34	6.1	10.50
KIT-5(150)-20TA	355	20.10	0.45	7.3	12.16

[a] SA: surface area; unit-cell parameters ($a_o = d_{111}\sqrt{3}$; PV: pore volume; PD: pore diameter; CD: cage diameter.

Figure 2 shows the nitrogen adsorption isotherms of KIT-5(100) functionalized with different amounts of TFA and pure KIT-5(100). All the samples exhibit a type IV adsorption isotherm with an H2 hysteresis loop, which is typically observed for the mesoporous samples with a cage-type pore structure. It must be noted that with an increase in the TFA content, the amount of nitrogen adsorbed decreases with the concomitant decrease of the height of the capillary condensation step, thereby indicating that the surface of the pores is occupied by the TFA molecules. The textural parameters of the TFA-functionalized samples derived from the nitrogen-adsorption isotherm are also given in Table 1. As can be seen in Table 1, the specific surface area, specific pore volume, and the cage diameter of the KIT-5(100) decrease with an increase in the loading of TFA inside the pore channels. The surface area decreases from 405 to 240 $m^2 g$, and the pore volume decreases from 0.31 to 0.22 $cm^3 g$ with an increasing amount of triflic acid in the KIT-5(100), whereas the pore diameter remains constant for all the samples. The capillary condensation is not shifted towards lower relative pressure when the amount of triflic acid in the silica framework of KIT-5 is increased. These results confirm that the TFA molecules are functionalized inside the mesochannels of the KIT-5(100) without blocking the pore entrance and can easily be accessible to the reactant molecules in the catalytic reactions.

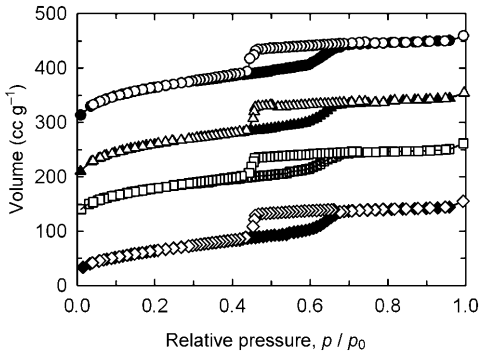

Figure 2. N_2 adsorption–desorption isotherms of (open symbols: desorption; closed symbols: adsorption): (○) KIT-5(100)-5TA, (△) KIT-5(100)-10TA, (□) KIT-5(100)-15TA, and (◇) KIT-5 (100)-20TA catalysts.

To check whether the TFA molecules are perfectly linked with the surface silanol groups on the internal pores of the KIT-5(100), the TFA-functionalized materials were characterized by FTIR spectroscopy. Figure 3 shows the FTIR spectra of KIT-5(100) functionalized with different amounts of TFA in comparison with the pure KIT-5(100). Both the TFA-functionalized and pure KIT-5(100) samples show four broad peaks at 2920–3830, 1550–1700, 730–875, and 400–550 cm^{-1}. The first two peaks are attributed to the OH stretching and vibration of hydroxyl groups and the physisorbed water molecules at the surface of the silica sample, respectively, whereas the latter two peaks are assigned to the stretching and the asymmetric stretching vibration mode

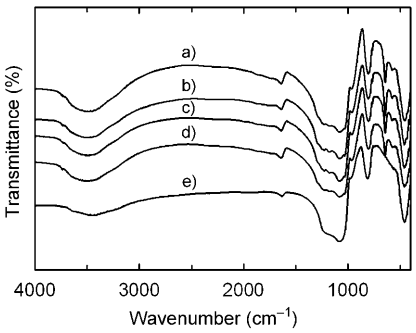

Figure 3. FTIR spectra of a) KIT-5(100)-20TA, b) KIT-5(100)-15TA, c) KIT-5(100)-10TA, d) KIT-5(100)-5TA, and e) KIT-5(100) catalysts.

of the Si-O-Si frameworks, respectively, in the amorphous wall structure of the KIT-5(100). A strong intense peak centered at 642 cm^{-1} and a small peak at 1030 cm^{-1} are observed only for the TFA-functionalized samples. The peak at 642 cm^{-1} is attributed to the C–S stretching, whereas the peak at 1030 cm^{-1} is assigned to the C–F stretching mode of the functionalized TFA molecules on the surface of the pore channels of KIT-5(100). It should be noted that all the TFA-functionalized KIT-5(100) samples also show a small peak centered at 1180 cm^{-1}, which corresponds to the S=O stretching more than the functionalized TFA molecules.[45–47] From these results, one can easily conclude that the TFA molecules are perfectly functionalized on the surface of the KIT-5(100) silica support without affecting its structural order, and the surface TFA groups can offer Brønsted acid sites for acid-catalyzed organic transformations.

TFA was also functionalized in KIT-5 silica with different pore diameters in an attempt to create superacidic mesoporous materials with a large pore diameter. Interestingly, support material with different pore diameters show a significant difference in the loading of TFA molecules in the mesoporous channels. The intensity of the C, F, and S peaks decreases with increasing the pore diameter of the support (Figure 4). This interesting feature can be explained as follows: the pore diameter of the support materials was controlled by simply increasing the synthesis temperature. It is quite expected that the materials prepared at higher temperature always have a lower number of surface silanol groups due to the enhancement of the cross-linking of the silanol groups, which are critical for the encapsulation of TFA molecules inside the mesoporous channels. This leads to a poor functionalization of TFA on the surface of the KIT-5 support with the largest pore and cage diameter.

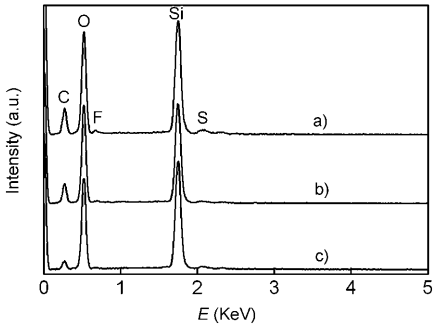

Figure 4. EDX patterns of a) KIT-5(100)-20TA, b) KIT-5(130)-20TA, and c) KIT-5(150)-20TA catalysts.

The structure of the TFA-functionalized KIT-5 support with different pore diameters was also analyzed by powder XRD measurements. The powder XRD patterns of TFA-functionalized mesoporous KIT-5 with different pore diameters are shown in Figure 5. All the samples exhibit well-ordered mesostructures, which is confirmed by the presence of sharp peaks at lower angles and several higher order peaks that can be indexed to the (111), (200), and (220) reflections of the cubic space group *Fm*3*m*. This indicates that the structural order of the material was not affected, even after the TFA functionalization. Moreover, a noticeable shift in the XRD diffraction peaks toward lower 2θ values is observed for the samples prepared at temperatures higher than 100 °C. This is simply due to the difference in the pore diameter of the KIT-5 supports that were prepared at a higher synthesis temperature. On the other hand, the unit-cell constant and the *d* spacing of the KIT-5(130)-20TA and KIT-5-(150)-20TA are much lower than those of their respective pristine supports.

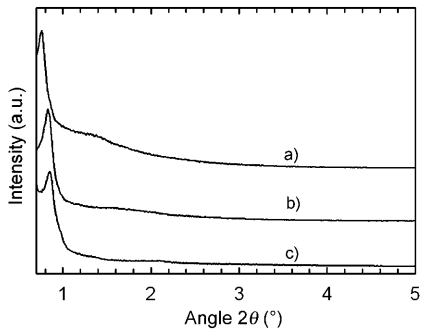

Figure 5. Powder XRD patterns of a) KIT-5(150)-20TA, b) KIT-5 (130)-20TA, and c) KIT-5(150)-20TA.

The porosity of the TFA-modified KIT-5 sample with different pore diameters was measured by N_2 adsorption–desorption isotherms. The N_2 adsorption–desorption isotherms and pore-size distribution of TFA-modified KIT-5 samples with different pore diameters are shown in Figures 6 and 7, respectively. All the samples possess a type IV isotherm with a sharp step at higher relative pressures and exhibit an H2 hysteresis loop. The shape of the capillary condensation step of the nitrogen-adsorption isotherms of the TFA-functionalized KIT-5 samples with different pore diameter is almost same as that of the pristine KIT-5 supports. This indicates that the pore structure of the materials was not significantly altered upon the functionalization of the surface of the KIT-5 with different pore diameters, which is quite consistent with the conclusion derived from the XRD data of these samples (Figure 5). As expected, the specific surface

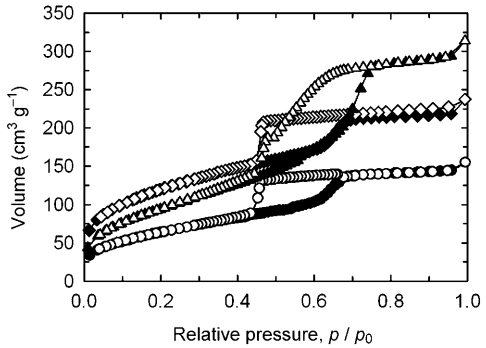

Figure 6. N_2 adsorption–desorption isotherms of (open symbols: desorption; closed symbols: adsorption): (○) KIT-5(100)-20TA, (□) KIT-5(130)-20TA, and (△) KIT-5(150)-20TA catalysts.

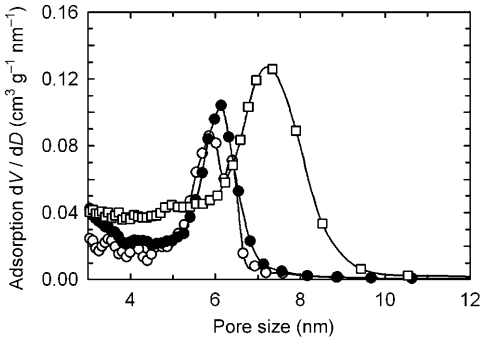

Figure 7. Adsorption pore-size distribution of (○) KIT-5(100)-20TA, (●) KIT-5(130)-20TA, and (□) KIT-5(150)-20TA catalysts.

area, specific pore volume, and the pore diameter of the TFA-functionalized samples are lower than those of the pristine KIT-5 support with different pore diameters. The reduction in the textural parameters of the support confirms that the TFA molecules completely cover the pore surface of the KIT-5 supports (Table 1). It must be noted that the reduction in the values of the textural parameters of the KIT-5(100) is more than those of the KIT-5(150) and KIT-5-(130). These results reveal that the density of the TFA groups on the KIT-5(100) support is higher than that of the KIT-5(130) and KIT-5(150), which is mainly due to the difference in the surface silanol groups on the pore surface of the KIT-5 support with different pore diameters. This result is also consistent with the conclusion derived from the high-resolution (HR) SEM-EDX data (Figure 4).

The coordination of TFA with the surface silanol groups of the KIT-5 with different pore diameters was also characterized by FTIR spectroscopy and the results are shown in Figure 8. The FTIR spectra of KIT-5(130)-20TA and KIT-5-(150)-20TA are fairly similar to that of KIT-5-(100)-20TA. All the samples show three well-resolved peaks that are centered at 642, 1030, and 1180 cm^{-1}. These peaks are typically assigned to the stretching vibration mode of the C–S, C–F, and S=O groups in the TFA molecules that are bonded with the surface silanol groups on the surface of the mesoporous

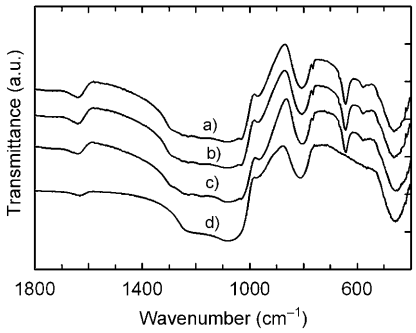

Figure 8. FTIR spectra of a) KIT-5(150)-20TA, b) KIT-5 (130)-20TA, c) KIT-5(100)-20TA, and d) KIT-5-100 catalysts.

support. It must be noted that these peaks are not observed for the sample without TFA functionalization.

The acidity of the KIT-5(100) functionalized with different amounts of TFA and of the TFA-functionalized KIT-5 support with different pore diameters was obtained by temperature-programmed desorption (TPD) of ammonia measurements, which helped us to quantify not only the number of acid sites but also the strength of the acid sites. It must be noted that the measurement was carried out up to a temperature of 300 °C as the TFA molecules bonded with the silanol groups on the surface of the KIT-5 support are believed to be decomposed at temperatures higher than 300 °C.[48–51] The ammonia TPD profiles of the TFA-functionalized KIT-5 support with different pore diameters are shown in Figure 9. As seen in Figure 9, all the samples show two

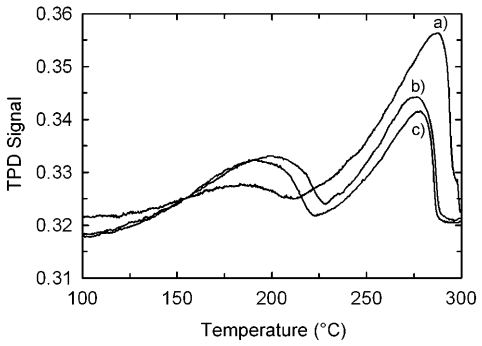

Figure 9. Ammonia TPD spectra of a) KIT-5(100)-20TA, b) KIT-5(130)-20TA, and c) KIT-5(150)-20TA catalysts.

broad signals in the temperature region of 140–220 and 230–300 °C, respectively, thereby revealing that the sample possess a wide distribution of acid sites with different acid strengths. The amount of the acidity of the TFA-functionalized KIT-5 support with different pore diameters is given in Table 2. Of the samples studied, KIT-5(100)-20TA showed the highest acidity, even though the pore diameter of the sample is much smaller than that of the other samples. As we discussed in the previous section, the higher acidity of the KIT-5(100)-20TA could be mainly due to the presence

Table 2. Effect of different catalysts and acidities for the synthesis of coumarin by the Pechmann reaction of resorcinol and ethyl acetoacetate.[a]

Catalysts	Conv.[b] [%]	Selectivity [%]	Total acidity [mmol g^{-1}]
KIT-5(100)	0	0	0
KIT-5(100)-5TA	38	23	0.37[c]
KIT-5(100)-10TA	42	78	0.45[c]
KIT-5(100)-15TA	67	93	1.09[c]
KIT-5(100)-20TA	77	96	1.47[c]
KIT-5(130)-20TA	73	82	1.39[c]
KIT-5(150)-20TA	70	74	1.30[c]
Mordenite	58	100	0.72[d]
HY	27	100	2.25[d]
H-ZSM	8	100	0.82[d]
AlSBA-15	16	100	0.36[d]
AlKIT-5	46	100	0.50[d]
AlMCM-41	0	0	0.36[d]
Recyclability of the catalyst			
1st cycle	71	91	–
2nd cycle	70	91	–

[a] Reaction conditions: resorcinol (10 mmol), ethyl acetoacetate (10 mmol), catalyst (0.1 g), reaction temperature 100 °C, reaction time 6 h. [b] Conversion with respect to resorcinol and based on GC analysis. [c] Temperature-programmed desorption measured at 300 °C. [d] Temperature-programmed desorption measured at 550 °C.

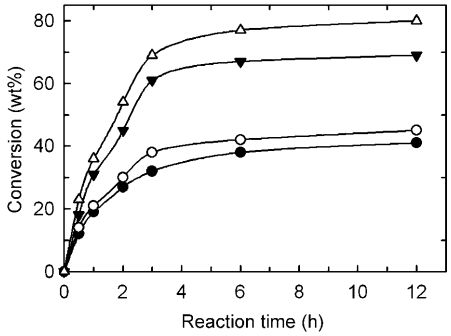

Figure 10. Effect of reaction time on conversion of resorcinol in the Pechmann reaction over different amounts of triflic acid loaded onto KIT-5(100)-20TA material. Curves: (●) KIT-5(100)-5TA, (○) KIT-5(100)-10TA, (▼) KIT-5(100)-15TA, and (△) KIT-5(100)-20TA catalysts. Reaction conditions: resorcinol (10 mmol), ethyl acetoacetate (10 mmol), catalyst (0.1 g), reaction temperature 100 °C.

of the highest number of silanol groups on the surface of the KIT-5(100) support, which would help to functionalize a huge number of TFA molecules on the surface, thereby resulting in a higher acidity.

It was also found that the peak maximum shifted towards a higher temperature as the pore diameter of the support was decreased, which indicates a slight enhancement of the average acid-site strength in the KIT-5(100)-20TA. The effect of the amount of TFA functionalization on the surface of KIT-5(100) on the acidity was also investigated. As can be seen in Table 2, the acidity of the materials increases with an increase in the amount of TFA functionalization on the surface of KIT-5(100). The acidity of KIT-5(100)-5TA is 0.37 mmol of NH_3 per gram which increases to 1.47 mmol of NH_3 per gram for KIT-5(100)-20TA. It is interesting to note that the acidity of KIT-5(100)-20TA is more than three times higher than that of the AlKIT-5(10) catalyst that was recently reported by us[52] and showed superior performance in the acetylation of aromatic compounds over zeolites and zeotype catalysts. Noteworthy is that when more than 20 wt% of TFA was used for functionalization, the textural parameters and the structural order of the materials were significantly deteriorated. From these characterization results, it can also be concluded that the KIT-5(100) that is prepared at a synthesis temperature of 100 °C is the best support for TFA functionalization.

Catalytic activity: To evaluate the catalytic activity, the Pechmann reaction has been carried out between resorcinol and ethyl acetoacetate using KIT-5 samples functionalized with different amounts of TFA molecules to produce the corresponding 7-hydroxy-4-methylcoumarin (Scheme 1). The results of the reactions as a function of reaction time are shown in Figure 10. The reaction was examined under solvent-free conditions for 12 h at 100 °C. The conversion of resorcinol was found to increase from 38 to 77% with an increase in the loading of TFA over KIT-5(100) from 5 to 20 wt% (Table 2). The product selectivity was also increased from 23 to 96% with an increase in the amount of TFA on the surface of KIT-5(100). This is mainly due to the fact that the total acidity of the material increases with an increase in the loading of TFA onto KIT-5(100) samples. The same reaction was examined over TFA-functionalized KIT-5 supports with different pore diameters such as KIT-5(100)-20TA, KIT-5(130)-20TA, and KIT-5(150)-20TA samples under identical reaction conditions. As expected, although the same amount of TFA was introduced onto the surface of the KIT-5 supports with different pore diameters, the conversion and product selectivity decreased with an increase in the pore diameter of the support (Table 2). This can be explained on the basis of incorporation of TFA onto the KIT-5 sample with different pore diameters, which dictates the acidity of the materials. The characterization results—including the HRSEM-EDX, nitrogen adsorption, and the acidity data described in the previous section—suggest that the amount of TFA functionalization on the surface of KIT-5(100)-20TA is higher than that of KIT-5(130)-20TA and KIT-5(150)-20TA. Therefore, the KIT-5(100)-20TA catalyst showed the highest activity in the synthesis of 7-hydroxy-4-methylcoumarin. Hence, further reactions were performed by using KIT-5(100)-20TA as catalyst.

The Pechmann reaction of resorcinol and ethyl acetoacetate was carried out under identical reaction conditions with different zeolites and metal-incorporated mesoporous materials. The results were compared with TFA-functionalized KIT-5 mesoporous materials (Table 2). It was observed that the catalytic activity of the 20 wt% TFA-loaded KIT-5 with different pore diameters is superior to the zeolites and metal-substituted mesoporous catalytic materials presented in Table 2. The conversion was found to be less than 10% for HZSM-5, whereas mordenite showed moderate activity, and no conversion was observed for the AlMCM-41 catalyst. Very recently we found that Al-incorporated KIT-5 material

showed higher catalytic activity for acetylation of veratrole and ring opening of epoxides than the zeolites and other metal-substituted mesoporous materials.[17,52] However, the catalytic activity of AlKIT-5 in the synthesis of coumarin derivatives is less than that of KIT-5(100)-20TA. This is mainly due to the presence of a huge number of acidic sites on the surface of the KIT-5 support that come from the TFA molecules and are easily available to the reactant molecules. In addition, the acidity of the TFA-loaded KIT-5 materials is much higher than that of AlKIT-5. These results clearly demonstrate the superior nature of TFA-functionalized KIT-5 catalyst in the synthesis of the derivatives of coumarin.

For the TFA-functionalized mesoporous supports, it is extremely important to study their stability, as it is widely believed that the functionalized TFA molecules may be leached out during the reaction. To test their catalyst stability, catalyst KIT-5(100)-20TA was separated from the reaction mixture and recycled for two consecutive reaction cycles. It was observed that the conversion is decreased marginally after the second recycle with almost no change in the selectivity of the product (Table 2). This shows that the catalyst is highly stable and could be regenerated several times under identical reaction conditions.

To optimize the weight of the catalyst in the reaction, the Pechmann reaction of resorcinol and ethyl acetoacetate was carried out over different amounts of KIT-5(100)-20TA as it was found to be the best catalyst under solvent-free conditions for the reaction time of 6 h. The results are shown in Figure 11. As expected, the total conversion and product selectivity increased from 61 to 77% and 75 to 96%, respectively, with an increase in the amount of catalyst from 0.025 to 0.10 g in the reaction mixture. It is reasonable to assume that the interaction of the reactant molecules with the active sites of the TFA-functionalized catalyst is significantly increased with an increase in the amount of catalyst in the reaction mixture. In addition, the availability of a higher number of active sites is also responsible for the higher activity when the amount of catalyst in the reaction mixture is increased. However, the reaction showed a marginal increase in the conversion when the catalyst amount was increased further to above 0.10 g.

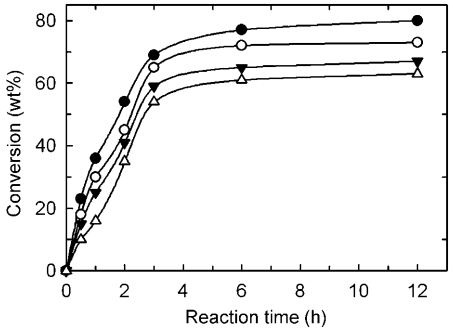

Figure 11. Effect of catalyst amount on the Pechmann reaction of resorcinol and ethyl acetoacetate over the KIT-5(100)-20TA catalyst. Reaction conditions: resorcinol (10 mmol) and ethyl acetoacetate (10 mmol), reaction temperature 100°C. Curves: (△) 0.025, (▼) 0.05, (○) 0.075, and (●) 0.1 g.

To study the efficiency of KIT-5(100)-20TA with respect to the reaction temperature, the Pechmann reaction of resorcinol and ethyl acetoacetate was carried out over KIT-5(100)-20TA (0.1 g) at different reaction temperatures of 40, 60, 80, and 100°C for the reaction time up to 6 h under solvent-free conditions. The different reaction times and the kinetic curves are shown in Figure 12. As expected, the conversion of resorcinol and product selectivity increase with an increase in the reaction temperature, thus indicating that the catalyst is quite stable and the reaction was free from diffusion limitation at higher temperatures. At 40°C, the conversion of resorcinol was 51%, even after 6 h with a product selectivity of 89%. From Figure 12, it can be seen that the rate of the reaction at lower temperature is rather slow, whereas the reaction is very fast at reaction temperatures above 80°C. The high conversion and product selectivity at higher temperatures clearly show that this reaction demands a high-activation energy and the acid sites are activated more at higher temperatures, which leads to a higher rate of attack of nucleophile (phenolic OH^-) to carbocation of β-ketoester (ethyl acetoacetate). Consequently, the conversion of resorcinol increases with an increase in the reaction temperature. However, there is no significant change in conversion in the temperature range 80–100°C, and the product selectivity was found to be almost the same in each case (89–96%).

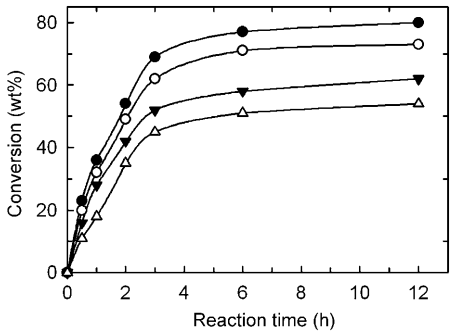

Figure 12. Effect of reaction temperature on the Pechmann reaction of resorcinol and ethyl acetoacetate over the KIT-5(100)-20TA catalyst. Reaction conditions: resorcinol (10 mmol) and ethyl acetoacetate (10 mmol), catalyst (0.1 g). Curves: (△) 40, (▼) 60, (○) 80, and (●) 100°C.

Conclusion

The surface of the highly ordered, three-dimensional, cage-type mesoporous silica with a cubic *Fm*3*m* closely packed symmetry (KIT-5) has been functionalized with superacid molecules, namely, TFA, using a simple wet impregnation method. The TFA molecules were also decorated on the surface of KIT-5 samples with different pore diameters, which

were prepared at different synthesis temperatures. The obtained materials have been characterized by sophisticated techniques such as XRD, N_2 adsorption, FTIR spectroscopy, and NH_3 TPD. The characterization results revealed that the TFA molecules are strongly bonded with the surface silanol groups of the KIT-5 supports. We also demonstrated that the acidity of the TFA-functionalized materials can be simply controlled by varying the amount of the TFA molecules on the surface. The synthesis temperature of the support also played a critical role in directing the acidity of the materials, as the hydrothermal process controls the surface silanol groups. The catalytic activities of the different amounts of TFA-functionalized KIT-5 support with different pore diameters have also been investigated for the synthesis of coumarin by means of the Pechmann reaction of ethyl acetoacetate and resorcinol under solvent-free conditions. The effects of various reaction parameters such as reaction time, reaction temperatures, and amount of catalyst have also been examined in detail. It has been observed that the KIT-5-(100)-20TA catalyst showed superior performance in the synthesis of coumarin with high conversion of resorcinol and high product selectivity of 4-methyl-7-hydroxycoumarin over zeolites and metal-substituted mesoporous catalytic materials. As these superacid-supported materials exhibit very high acidity with a well-ordered porous structure, the materials could be used for various other acid-catalyzed transformations that require high acidity.

Experimental Section

Materials: The triblock copolymer (Pluronic F127 (EO97 PO69 EO97), $M_r = 12500$) was obtained from Sigma Co. and used as the structure-directing agent. Tetraethylorthosilicate (TEOS) was purchased from Aldrich and used as a source for silicon. TFA was purchased from Aldrich. Resorcinol (99%) and ethyl acetoacetate (99%) were obtained from Wako Chemicals and used as received without further purification.

Syntheses of KIT-5 catalyst with various pore diameters: The mesoporous KIT-5 support with different pore diameters was synthesized using Pluronic F127 as the template in an acidic medium at different synthesis temperatures. In a typical synthesis, F127 (2.5 g), distilled water (120 g), and concentrated hydrochloric acid (5.25 g, 35 wt% HCl) were mixed together and stirred for a few hours to attain a homogenous solution. TEOS (12 g) was quickly added to this mixture under stirring at 45 °C. The mixture was stirred at 45 °C for 24 h for the formation of the mesostructured product. Subsequently, the reaction mixture was heated for 24 h at 100 °C under static conditions for hydrothermal treatment, filtered, and then dried at 100 °C without washing. Another set of samples was prepared according to the above procedure except by variation of the synthesis temperature from 100 to 150 °C. The samples were calcined in air at 550 °C and labeled KIT-5(T); T denotes the synthesis temperature. The following molar gel composition was used: TEOS/F127/HCl/H_2O 1:0.0035:0.88:119.

Functionalization of TFA over KIT-5 with different pore diameters: The mesoporous KIT-5(T) was functionalized with TFA by the postsynthetic method. The reaction pathway is shown in Scheme 2. In a typical synthesis, TFA (0.03 mol) was added to a mixture of toluene and KIT-5 under a nitrogen atmosphere and heated to reflux at 90 °C for 2 h. Subsequently, the mixture was cooled, filtered, washed with acetone, and dried at 100 °C for 6 h. The unreacted TFA was removed by soxhlet extraction by using a mixture of dichloromethane (100 g) and diethyl ether (100 g) per gram of the catalyst for 24 h. Then the solid product was dried at 100 °C

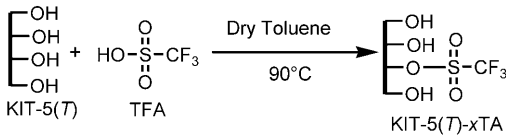

Scheme 2. Synthesis of TFA-modified KIT-5 mesoporous materials.

for 10 h. A first set of samples was prepared by varying the amount of TFA from 5 to 20 wt% over KIT-5(100) and were denoted as KIT-5-(100)-xTA; x denotes the weight percentage of TFA. A second series of the samples was prepared by using a fixed wt% of TFA of 20 while varying the pore diameter of the mesoporous KIT-5 support. These samples are denoted KIT-5(T)-20TA; T denotes the synthesis temperature of the mesoporous support.

Characterization of the catalysts: The powder X-ray diffraction patterns of KIT-5 and TFA-functionalized KIT-5 supports were collected using a Rigaku diffractometer with $Cu_{K\alpha}$ ($\lambda = 0.154$ nm) radiation. The diffractograms were recorded in the 2θ range of 0.7–10° with a 2θ step size of 0.01° and a step time of 6 s. Nitrogen-adsorption and -desorption isotherms were measured at −196 °C using a Quantachrome Autosorb 1 sorption analyzer. The samples were outgassed for 6 h at 150 °C under vacuum in the degas port of the adsorption analyzer. The specific surface area was obtained from the adsorption branch of the isotherm in the relative pressure range of 0.05–0.18 by using the BET equation. The position of the maximum on pore-size distribution is referred to as the pore diameter, which was calculated from the adsorption branch of the nitrogen isotherms using the Barrett–Joyner–Halenda (BJH) method. The diameter of the cages in KIT-5 materials was calculated using Equation (1), which was recently proposed by Ravikovitch et al.:[53]

$$D_{me} = a(6\,\varepsilon_{me}/\pi\nu)^{1/3} \quad (1)$$

in which D_{me} is the diameter of the cavity of a cubic unit cell of length a, ε_{me} is the volume fraction of a regular cavity, and ν is the number of cavities present in the unit cell (for the $Fm3m$ space group, $\nu = 4$). The average wall thickness of the materials (h) was calculated using Equation (2), which was derived from the mesoporosity and D_{me}:

$$h = [(D_{me}/3)(1-\varepsilon_{me})]/\varepsilon_{me} \quad (2)$$

The FTIR spectra of TFA-functionalized KIT-5 materials were recorded in the range of 400–4000 cm^{-1} with a resolution of 4 cm^{-1} using a Thermo Nicolet instrument (model Nexus 870) and a KBr pellet was taken as reference. The temperature-programmed desorption of ammonia (NH_3 TPD) was carried out using a Micromeritics Autochem 2910 instrument. A fresh sample (approximately 30 mg) was placed in a U-shaped, flow-through, quartz microreactor and then inserted into the analysis port of the instrument. The sample cell was then covered with a computer-controlled high-temperature furnace. Prior to each analysis, the catalyst was activated at 300 °C for 6 h under He flow (20 mL min^{-1}) and then cooled to 100 °C before being exposed to ammonia for about 1 h. The sample was flushed again with He until the baseline was reached in the thermal conductivity detector (TCD) attached to the instrument to remove any physisorbed ammonia. The desorption profile was recorded by increasing the temperature of the sample from 100 to 300 °C at a heating rate of 5 °C per min.

Catalytic reactions: Coumarin was synthesized by the Pechmann reaction of resorcinol and ethyl acetoacetate under liquid-phase and solvent-free conditions (Scheme 1) using TFA-functionalized KIT-5 catalysts. The reaction was carried out in a 50 mL two-necked round-bottomed flask equipped with a condenser and an additional port to withdraw samples at regular intervals under continuous stirring. The temperature of the above assembly was maintained by placing it in an oil bath equipped with a thermostat. In a typical reaction, the catalyst (0.10 g), resorcinol (1.1 g, 10 mmol), and ethyl acetoacetate (1.3 g 10 mmol) were mixed and heated at 100 °C for several hours. The samples were collected at regular intervals and analyzed periodically by using a Shimadzu gas chromatograph

GC-2010 with a TCD detector and a DB-5 capillary column. The products were confirmed by GC–MS analysis. To optimize the reaction conditions, the reactions were carried out using a different amount of TFA loading on the support, weight of the catalyst, reaction temperature, and reaction time. The products were also analyzed by GC. The product was identified by ^{1}H and ^{13}C NMR spectroscopic techniques. Product 7-hydroxy 4-methyl coumarin: m.p. 186–189 °C (petroleum ether/ethyl acetate 2:1); ^{1}H NMR (200 MHz, $CDCl_3$ + 4 drops of $[D_6]DMSO$): $\delta = 9.68$ (s, 1H), 7.29–7.33 (m, 1H), 6.68–6.72 (m, 2H), 5.92–5.95 (m, 1H), 2.27 ppm (s, 3H); ^{13}C NMR (100 MHz, $CDCl_3$) $\delta = 161.20$, 161.12, 154.97, 153.04, 125.70, 112.99, 110.43, 102.6, 18.38 ppm.

Recyclability of the catalysts: To check the recyclability of the catalyst KIT-5(100)-20TA in the above-mentioned reaction, the catalyst was separated by filtration from the hot reaction mixture. The catalyst was washed three times with 1,2-dichloromethane and dried in the oven at 100 °C for 12 h. In the recycling reactions, the weight ratios of the catalyst and reactants were kept constant.

Acknowledgements

This work was supported by the Ministry of Education, Culture, Sports, Science, and Technology (MEXT) under the Strategic Program for Building an Asian Science and Technology Community Scheme and World Premier International Research Center (WPI) Initiative on Materials Nanoarchitectonics, MEXT, Japan. A.V. thanks Mr. H. Oveisi for the technical support.

[1] C. T. Kresge, M. E. Leonowicz, W. J. Roth, J. C. Vartuli, J. S. Beck, *Nature* **1992**, *359*, 710–712.
[2] A. Corma, *Chem. Rev.* **1997**, *97*, 2373–2420.
[3] M. Hartmann, A. Vinu, *Langmuir* **2002**, *18*, 8010–8016.
[4] A. Vinu, V. Murugesan, M. Hartmann, *J. Phys. Chem. B* **2004**, *108*, 7323–7330.
[5] D. Zhao, Q. Huo, J. Feng, B. F. Chmelka, G. D. Stucky, *J. Am. Chem. Soc.* **1998**, *120*, 6024–6036.
[6] Q. Zhang, K. Ariga, A. Okabe, T. Aida, *J. Am. Chem. Soc.* **2004**, *126*, 988–989.
[7] A. Vinu, V. Murugesan, O. Tangermann, M. Hartmann, *Chem. Mater.* **2004**, *16*, 3056–3065.
[8] S. Che, A. E. G. Bennet, Y. Yokoi, K. Sakamoto, H. Kunieda, O. Terasaki, T. Tatsumi, *Nat. Mater.* **2003**, *2*, 801–805.
[9] Q. Huo, R. Leon, P. M. Petroff, G. D. Stucky, *Science* **1995**, *268*, 1324–1327.
[10] A. Vinu, V. Murugesan, M. Hartmann, *Chem. Mater.* **2003**, *15*, 1385–1393.
[11] Q. Huo, D. I. Margolese, U. Ciesla, D. G. Demuth, P. Feng, T. Gier, P. Sieger, A. Firouzi, B. F. Chmelka, F. Schuth, *Chem. Mater.* **1994**, *6*, 1176–1191.
[12] D. Zhao, J. Feng, Q. Huo, N. Melosh, G. H. Fredickson, B. F. Chmelka, G. D. Stucky, *Science* **1998**, *279*, 548–552.
[13] A. Vinu, T. Krithiga, V. Murugesan, M. Hartmann, *Adv. Mater.* **2004**, *16*, 1817–1821.
[14] A. Vinu, V. Murugesan, W. Bohlmann, M. Hartmann, *J. Phys. Chem. B* **2004**, *108*, 11496–11505.
[15] A. Vinu, D. P. Sawant, K. Ariga, K. Z. Hossain, S. B. Halligudi, M. Hartmann, M. Nomura, *Chem. Mater.* **2005**, *17*, 5339–5345.
[16] A. Vinu, P. Srinivasu, M. Miyahara, K. Ariga, *J. Phys. Chem. B* **2006**, *110*, 801–806.
[17] P. Srinivasu, S. Alam, V. V. Balasubramanian, S. Velmathi, D. P. Sawant, W. Bohlmann, S. P. Mirajkar, K. Ariga, S. B. Halligudi, A. Vinu, *Adv. Funct. Mater.* **2008**, *18*, 640–651.
[18] S. A. Bagshaw, E. Prouzet, T. J. Pinnavaia, *Science* **1995**, *269*, 1242–1244.
[19] F. Kleitz, D. Liu, G. M. Anilkumar, I.-S. Park, L. A. Solovyov, A. N. Shmakov, R. Ryoo, *J. Phys. Chem. B* **2003**, *107*, 14296–14300.
[20] A. Vinu, M. Miyahara, K. Z. Hossain, M. Takahashi, V. V. Balasubramanian, T. Mori, K. Ariga, *J. Nanosci. Nanotechnol.* **2007**, *7*, 828–832.
[21] A. Vinu, M. Miyahara, V. Sivamurugan, T. Mori, K. Ariga, *J. Mater. Chem.* **2005**, *15*, 5122–5127.
[22] M. Chidambaram, D. Curulla-Ferre, A. P. Singh, B. G. Anderson, *J. Catal.* **2003**, *220*, 442–456.
[23] D. O. Bennardi, G. P. Romanelli, J. C. Autino, L. R. Pizzio, *Appl. Catal. A* **2007**, *324*, 62–68.
[24] J. A. Melero, R. Van Grieken, G. Morales, *Chem. Rev.* **2006**, *106*, 3790–3812.
[25] M. A. Jackson, I. K. Mbraka, B. H. Shanks, *Appl. Catal. A* **2006**, *310*, 48–53.
[26] Y. Gu, A. Karam, F. Jerome, J. Barrault, *Org. Lett.* **2007**, *9*, 3145–3148.
[27] R. O'Kennedy, R. D. Thornes, Coumarins: Biology, *Applications and Mode of Action*, Wiley, New York, **1997**, pp. 23–60.
[28] L. A. Singer, N. P. Long, *J. Am. Chem. Soc.* **1966**, *88*, 5213–5219.
[29] M. Zahradnik, *The Production and Application of Fluorescent Brightening Agents*, Wiley, New York, **1992**, pp. 78–81.
[30] R. D. H. Murray, J. Mendez, S. A. Brown, *The Natural Coumarins, Occurrence*, Wiley, New York, **1982**.
[31] H. Von Pechmann, C. Duisberg, *Chem. Ber.* **1884**, *17*, 929.
[32] A. Ramani, B. M. Chanda, S. Velu, S. Sivansaker, *Green Chem.* **1999**, *1*, 163–165.
[33] F. Bigi, L. Chesini, R. Maggi, G. Sartori, *J. Org. Chem.* **1999**, *64*, 1033–1035.
[34] D. S. Bose, A. P. Rudradas, M. Hari Babu, *Tetrahedron Lett.* **2002**, *43*, 9195–9197.
[35] S. K. De, R. A. Gibbs, *Synlett* **2005**, 1231–1233.
[36] G. V. M. Sharma, J. J. Reddy, P. S. Lakshmi, P. R. Krishna, *Tetrahedron Lett.* **2005**, *46*, 6119–6121.
[37] M. K. Potdar, S. S. Mohile, M. M. Salunkhe, *Tetrahedron Lett.* **2001**, *42*, 9285–9287.
[38] Y. Gu, J. Zhang, Z. Duan, Y. Deng, *Adv. Synth. Catal.* **2005**, *347*, 512–516.
[39] A. D. Hoz, M. Andres, E. Vazquez, *Synlett* **1999**, 602–604.
[40] D. A. Chaudhari, *Chem. Ind.* **1983**, 568.
[41] E. A. Gunnewegh, A. J. Hoefnagel, H. van Bekkum, *J. Mol. Catal. A* **1995**, *100*, 87–92.
[42] S. Frere, V. Thiery, T. Besson, *Tetrahedron Lett.* **2001**, *42*, 2791–2794.
[43] T. Li, Z. Zhang, F. Yang, C. Fu, *J. Chem. Res.* **1998**, 38–39.
[44] J. C. Rodríguez-Domínguez, G. Kirsch, *Tetrahedron Lett.* **2006**, *47*, 3279–3281.
[45] G. Herzberg, *Infrared and Raman Spectra of Polyatomic Molecules*, Van Nostrand, New York, **1945**, p. 285.
[46] L. J. Bellamy, *The Infrared Spectra of Complex Molecules*, Wiley, New York, **1960**, p. 328.
[47] J. Pouchert, *The Aldrich Library of IR Spectra*, 3rd ed., Springer, Heidelberg, **1981**, p. 533.
[48] R. D. Howells, J. D. Mc Cown, *Chem. Rev.* **1977**, *77*, 69–92.
[49] A. N. Parvulescu, B. C. Gagea, M. Alifanti, V. Parvulescu, V. I. Parvulescu, S. Nae, A. Razus, G. Poncelet, P. Grange, *J. Catal.* **2001**, *202*, 319–323.
[50] N. C. Marziano, L. D. Ronchin, C. Tortato, A. Zingales, A. A. Sheikh-Osman, *J. Mol. Catal. A* **2001**, *174*, 265–277.
[51] Q. Zhou, J. H. Yang, G. M. Dong, M. Y. Huang. Y. Y. Jiang, *J. Mol. Catal. A* **2000**, *159*, 85–87.
[52] R. Chakravarti, H. Oveisi, P. Kalita, R. R. Pal, S. B. Halligudi, M. L. Kantam, A. Vinu, *Microporous Mesoporous Mater.* **2009**, 123, 338–344.
[53] P. I. Ravikovitch, A. V. Neimark, *Langmuir* **2002**, *18*, 1550–1560.

Received: September 14, 2009
Published online: January 19, 2010

